Human Molecular Genetics, 2013, Vol. 22, No. 12 **2510–2519**
doi:10.1093/hmg/ddt102
Advance Access published on February 27, 2013

Role of Gα(olf) in familial and sporadic adult-onset primary dystonia

Satya R. Vemula[1], Andreas Puschmann[2], Jianfeng Xiao[1], Yu Zhao[1], Monika Rudzińska[3], Karen P. Frei[4], Daniel D. Truong[4], Zbigniew K. Wszolek[5] and Mark S. LeDoux[1,*]

[1]Departments of Neurology, and Anatomy & Neurobiology, University of Tennessee Health Science Center, Memphis, TN 38163, USA [2]Department of Neurology, Skåne University Hospital, Lund University, Lund, Sweden [3]Department of Neurology, Jagiellonian University Medical College in Krakow, Krakow, Poland [4]Parkinson's & Movement Disorder Institute, Fountain Valley, CA 92708, USA [5]Department of Neurology, Mayo Clinic Jacksonville, Jacksonville, FL 32224, USA

Received December 19, 2012; Revised February 10, 2013; Accepted February 14, 2013

The vast majority of patients with primary dystonia are adults with focal or segmental distribution of involuntary movements. Although ∼10% of probands have at least one first- or second-degree relative to dystonia, large families suited for linkage analysis are exceptional. After excluding mutations in known primary dystonia genes (*TOR1A*, *THAP1* and *CIZ1*), whole-exome sequencing identified a *GNAL* missense mutation (c.682G>T, p.V228F) in an African-American pedigree with clinical phenotypes that include cervical, laryngeal and hand-forearm dystonia. Screening of 760 subjects with familial and sporadic primary dystonia identified three Caucasian pedigrees with *GNAL* mutations [c.591dupA (p.R198Tfs*13); c.733C>T (p.R245*); and c.3G>A (p.M1?)]. These mutations show incomplete penetrance. Our findings corroborate those of a recent study which used whole-exome sequencing to identify missense and nonsense *GNAL* mutations in Caucasian pedigrees of mixed European ancestry with mainly adult-onset cervical and segmental dystonia. *GNAL* encodes guanine nucleotide-binding protein G(olf), subunit alpha [Gα(olf)]. Gα(olf) plays a role in olfaction, coupling D1 and A2a receptors to adenylyl cyclase, and histone H3 phosphorylation. African-American subjects harboring the p.V228F mutation exhibited microsmia. Lymphoblastoid cell lines from subjects with the p.V228F mutation showed upregulation of genes involved in cell cycle control and development. Consistent with known sites of network pathology in dystonia, immunohistochemical studies indicated that Gα(olf) is highly expressed in the striatum and cerebellar Purkinje cells, and co-localized with corticotropin-releasing hormone receptors in the latter.

INTRODUCTION

Dystonia, defined as a syndrome of involuntary, sustained muscle contractions affecting one or more sites of the body, frequently causing twisting and repetitive movements or abnormal postures, is a genetically and clinically heterogeneous movement disorder (1). Dystonias are categorized by etiology (primary, secondary, dystonia-plus, and heredodegenerative diseases with dystonia), age of onset [early (<20 years) or late (≥20 years)] and anatomical distribution (focal, segmental, multifocal, hemidystonia or generalized) (1,2). Most cases of primary dystonia begin in adults and primary adult-onset dystonia is more common in females (2,3). Cervical dystonia (CD) or spasmodic torticollis is the most common form of focal dystonia, characterized by involuntary contractions of the neck muscles producing abnormal posturing of the head upon the trunk (4). In the USA, primary dystonia may be less common among African-Americans than Caucasians (5,6). Genetic factors contribute to the pathogenesis of adult-onset primary dystonia since 10% of patients have one or more affected first- or second-degree relatives (2,7). Familial and sporadic dystonia appear to share the same genetic underpinnings (8).

To date, six genes (*TOR1A*, *THAP1*, *CIZ1*, *ANO3, GNAL* and *TUBB4A*) and additional genetic loci (DYT13 and

*To whom correspondence should be addressed at: University of Tennessee Health Science Center, Department of Neurology, 855 Monroe Avenue, Link Building-Suite 415, Memphis, TN 38163, USA. Tel: +901 4481662; Fax: +901 4487440; Email: mledoux@uthsc.edu

DYT21) have been linked to primary dystonia (9–18). Mutations in *TOR1A* are typically associated with early-onset generalized dystonia, whereas mutations in *THAP1* most commonly cause segmental craniocervical dystonia. Mutations in *CIZ1* have only been reported in patients with adult-onset cervical dystonia (12). In aggregate, these genes account for <10% of adult-onset cases of primary dystonia. Although adult-onset primary dystonia has a considerable heritable component, penetrance is reduced and the identification of genetic etiologies had been hampered by the availability of large pedigrees that were sufficiently powered for linkage analysis. With the advent of whole-exome sequencing, smaller pedigrees have proven suitable for the identification of sequence variants (SVs) causally associated with dystonia.

While the contributions of *TOR1A* and *THAP1* to primary dystonia are well established, the roles of *CIZ1*, *ANO3*, *TUBB4A* and *GNAL* have not been demonstrated in independent patient cohorts. In the present study, we confirm that familial adult-onset primary dystonia can result from mutations in *GNAL*, which encodes guanine nucleotide-binding protein, alpha activating activity polypeptide, olfactory type (Gα(olf), Golfalpha), a key player in signal transduction within the olfactory neuroepithelium and basal ganglia (19,20).

RESULTS

Linkage analysis and exome sequencing

GNAL mutations were identified in the four independent pedigrees (Fig. 1). The largest family (A) was employed for linkage analysis and whole-exome sequencing. As previously described (6), the members of this pedigree reported ages of onset from 45 to 63 years (Table 1). All affected subjects in Families A, B, C and D had dystonia and varying degrees of objective microsmia with otherwise normal neurological examinations. In particular, no subject showed clinical evidence of ataxia, spasticity, oculomotor abnormalities, Parkinsonism or neuropathy.

Eighteen subjects from Family A were genotyped with the Illumina HumanLinkage-24 Bead Chip. Call rates were over 99.6% for all 18 samples and reproducibility was 100% for 6 samples subjected to technical replication (Supplementary Material, Table S1). SNP genotypes were analyzed with Superlink-Online SNP version 1.0 (21). The highest multipoint LOD score was 1.10 (Supplementary Material, Table S2). LOD scores of 1 or less were obtained within the DYT7, DYT13 and DYT21 loci.

Whole-exome capture and massively parallel sequencing was performed on two definitely affected and one unaffected subject from Family A. Over 99.5% of exons were covered at ≥2× and over 96.1% of exons were covered at ≥20× (Supplementary Material, Table S3). After filtering and elimination of read errors with Sanger sequencing, three potentially pathological SVs were common to the two affected subjects and absent from the unaffected subject. However, only a single SV co-segregated with dystonia in Family A (*GNAL*; c.682G>T, p.V228F).

Linkage analysis of Family A using c.682G>T *GNAL* genotypes with penetrance values of 0.5 and 0.99 yielded LOD scores of 2.90 and 4.03, respectively, at rs879588 (Supplementary Material, Table S4; Fig. S1). This SNP is located near *GNAL* on Chr 18p11.2. Haplotype analysis of Chr 18p showed that SNPs near *GNAL* co-segregated with c.682G>T in subjects with dystonia (Supplementary Material, Fig. S2). *In silico* analyses with ClustalW2 (22), Polyphen-2 (23), SIFT (24) and MutationTaster (25) indicated that c.682G>T (p.V228F) altered a highly conserved amino acid and was disease causing (Supplementary Material, Table S5).

Mutation screening and *in silico* analysis

High-resolution melting (7,12) and Sanger sequencing were used for *GNAL* mutation screening in 760 subjects with mainly CD and 768 neurologically-normal controls (Supplementary Material, Tables S6–S7). Five additional novel SVs were identified and *in silico* analyses predicted three of these variants to be pathogenic: c.591dupA (p.R198Tfs*13), c.733C>T (p.R245*) and c.3G>A (p.M1?). Two (c.591dupA and c.733C>T) of these three mutations are predicted to cause premature stop codons and probably induce nonsense-mediated decay (NMD), while c.3G>A disrupts the start codon of Isoform 2.

Clinical characteristics of subjects with *GNAL* mutations

As seen in Table 1, 9 of the 11 affected subjects from Families A–D were female. The age of onset ranged from 37 to 63 years. The mean age of onset was 45 years. Among the 11 affected subjects, 7 had isolated focal dystonia manifest as CD. There was a single subject with generalized dystonia and three with segmental dystonia. Seven subjects had a dystonic head tremor.

GNAL mutations show incomplete penetrance. Unaffected carriers were present in Families A, B and D (Fig. 1; and Supplementary Material, Table S8). Of the 14 unaffected carriers included in this study, there were five males and nine females. The ages of unaffected carriers ranged from 9 to 51 years with a mean of 29 years.

Role of Gα(olf) in olfaction

When data from all four families were grouped together, the differences in mean University of Pennsylvania Smell Identification Test (UPSIT) scores ± standard error of the mean among manifesting carriers ($n = 7$, 30.8 ± 3.1), non-manifesting carriers ($n = 8$, 33.7 ± 2.8) and non-carrier neurologically normal family members ($n = 14$, 35.1 ± 3.7) were not significant (26). However, an independent one-tailed *t*-test restricted to data from Family A indicated that manifesting and non-manifesting mutation carriers ($n = 6$, 25.5 ± 2.9) had lower UPSIT scores than non-carrier neurologically normal family members ($n = 5$, 33.0 ± 1.1; $P < 0.026$). Microsmia was not self-reported in Families A–D, but only detected through objective UPSIT testing.

Relative expression of *GNAL*

GNAL has three isoforms. Isoform 1 (NM_182978.3) is the longest, whereas Isoform 2 (NM_001142339.2) is the major

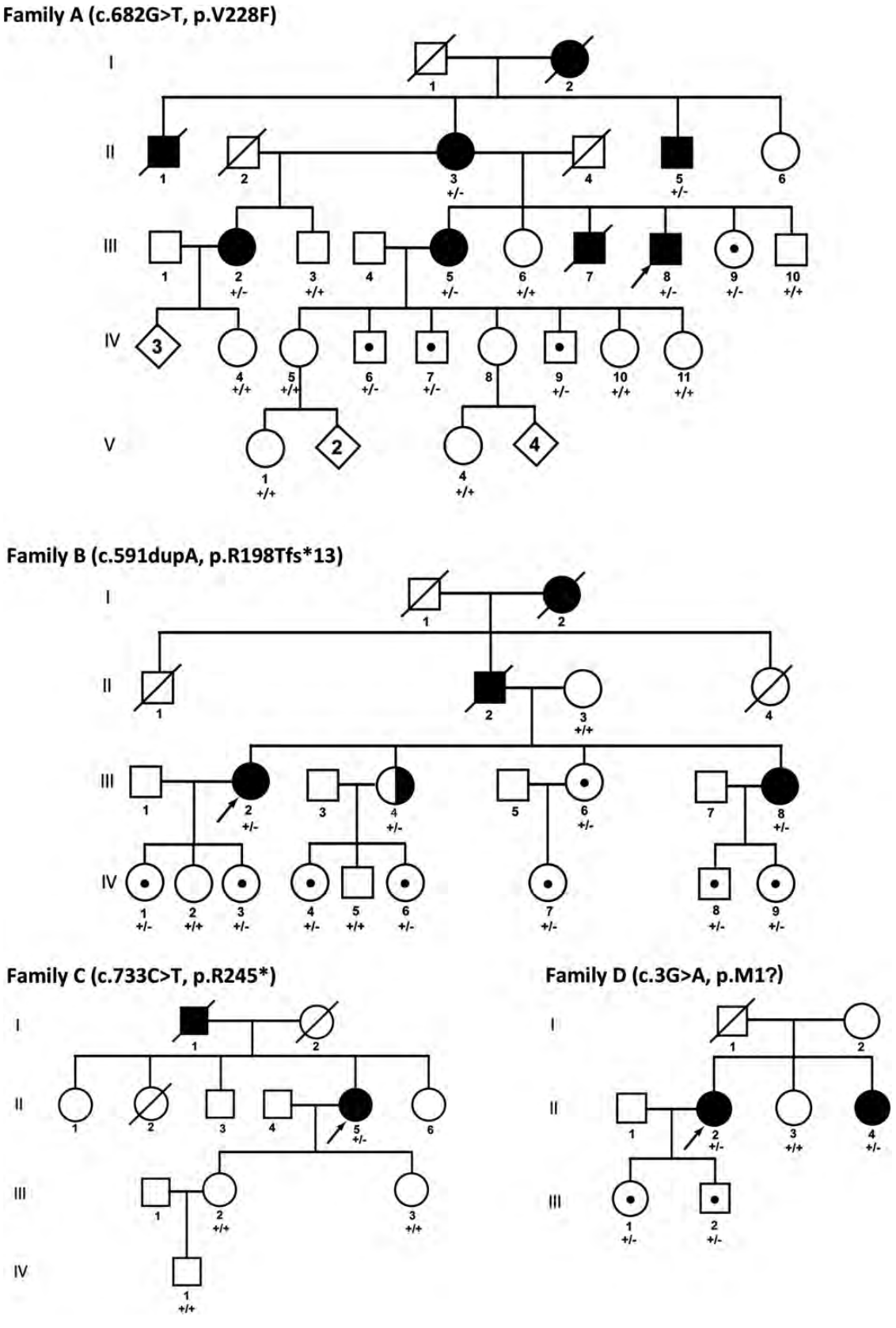

Figure 1. Family pedigrees. Filled symbols, definitely affected. Half-filled symbols, probably affected. Symbols with central dots, unaffected carriers. Arrows, probands. *GNAL* genotypes: wild-type (+/+) and heterozygous mutant (+/−). The genotypes of three subjects from Family B have recently been reported (13).

Table 1. GNAL mutant phenotypes

Subject	Age	Gender	Age of onset	Anatomical distribution	*GNAL* mutation
A-II-03	80	F	50	Segmental dystonia (cervical[a], blepharospasm, oromandibular, spasmodic dysphonia), anosmia	c.682G>T (p.V228F)
A-II-05	78	M	NA	Segmental dystonia (spasmodic dysphonia, hand-forearm)	c.682G>T (p.V228F)
A-III-02	67	F	63	Generalized dystonia (cervical[a], hand-forearm, lower limb)	c.682G>T (p.V228F)
A-III-05	55	F	50	Segmental dystonia (cervical[a], oromandibular, spasmodic dysphonia, hand-forearm), moderate microsmia	c.682G>T (p.V228F)
A-III-08	49	M	45	cervical dystonia[a], severe microsmia	c.682G>T (p.V228F)
B-III-02	56	F	38	cervical dystonia[a]	c.591dupA (p.R198Tfs*13)
B-III-08	46	F	37	cervical dystonia[a]	c.591dupA (p.R198Tfs*13)
B-III-04	54	F	NA	cervical dystonia (probable)	c.591dupA (p.R198Tfs*13)
C-II-05	55	F	45	cervical dystonia, moderate microsmia	c.733C>T (p.R245*)
D-II-02	55	F	40	cervical dystonia	c.3G>A (p.M1?)
D-II-04	44	F	41	cervical dystonia[a]	c.3G>A (p.M1?)

[a]Dystonic head tremor.

isoform (Fig. 2). GenBank (http://www.ncbi.nlm.nih.gov/genbank/) cDNAs whose sequences support the existence of Isoform 3 have not been found in brain. Relative expression of Isoforms 1 and 2 was examined in human brain and leukocytes using quantitative RT–PCR (QRT–PCR; Supplementary Material, Table S9). Overall *GNAL* expression was highest in striatum and fetal whole brain, whereas relative expression of Isoform 2 to 1 was highest in striatum and cerebral cortex. Suggestive of NMD, overall leukocyte expression of *GNAL* was reduced in one subject from Family B (c.591dupA). We were unable to detect Isoform 1 in leukocytes. The c.3G>A mutation in Family D had no apparent effect on leukocyte expression of *GNAL*.

Immunohistochemistry of Gα(olf) in the rat central nervous system

Since previous studies of Gα(olf) had focused on the olfactory bulb and striatum, we performed immunohistochemistry with a rabbit polyclonal anti-Gα(olf) antibody to obtain a more complete picture of Gα(olf)'s distribution in the rat central nervous system (Supplementary Material, Table S10). Gα(olf) immunoreactivity (IR) was present in olfactory bulb, striatum, thalamus, substantia nigra and cerebellum at P14 and in adult rat brains (Fig. 3). In cerebellum, Gα(olf)-IR was most prominent in Purkinje cells with weaker IR in granule cells. At P14, Gα(olf)-IR was seen throughput the dendritic arbor of Purkinje cells. However, in adult cerebellum, Gα(olf)-IR was largely restricted to the soma and proximal dendrites of Purkinje cells. In Purkinje cells, Gα(olf) co-localized with CRH-RI/II, but not PMCA4. At P14, Gα(olf)-IR was concentrated in the somas and proximal dendrites of medium spiny and cholinergic neurons within the striatum. In adult brain, more diffuse striatal Gα(olf)-IR was apparent. Gα(olf)-IR was localized to ChAT positive in striatal neurons at P14. However, in adult rat brain, Gα(olf)-IR in striatal cholinergic neurons was weak. At P14, Gα(olf)-IR was prominent in both dopaminergic and non-dopaminergic neurons of the substantial nigra. In adult rat brain, Gα(olf)-IR remained robust in TH-positive neurons of the substantia nigra but was less conspicuous in TH-negative neurons.

Gene expression analysis

Given the diverse role of G-proteins in regulating myriad cellular processes, gene expression studies were performed to identify pathways possibly dysregulated by mutant Gα(olf) [p.V228F]. These experiments employed RNA derived from lymphoblastoid cell lines established for four affected carriers (three females and one male) and four non-carriers (three females and one male) from Family A. In comparison to endogenous control and other dystonia-associated genes, *GNAL* was expressed at relatively low levels in lymphoblastoid cell lines (Supplementary Material, Table S11). However, the p.V228F mutation elicited highly reproducible effects on the transcriptome (Supplementary Material, Table S12).

In total, 82 genes were upregulated and 29 were downregulated (Supplementary Material, Tables S13 and S14; Fig. S3). Our gene set enrichment identified 15 significant KEGG pathways (Supplementary Material, Table S15). Upregulated pathways included Wnt signaling (*LRP5, PLCB2 and FZD3*), cytokine–cytokine interactions (*IL17RB, TNFRSF14* and *CXCL10*) and arrhythmogenic right ventricular cardiomyopathy (*ACTN1*, *DMD* and *LMNA*). Top canonical pathways upregulated, as indicated by IPA, included vitamin D receptor/retinoic acid X receptor (VDR/RXR) and G-protein receptor-coupled signaling (*EMR2, FZD3, OXTR, PDE6G, PLCB2* and *PRKCE*) (Supplementary Material, Tables S16 and S17). The top dysregulated networks were involved in cell cycle control, development, cell death and cellular proliferation (Table 2).

DISCUSSION

Previous work from several groups had suggested that a dystonia-associated gene resides on Chr 18p (16,27–33). In 1996, Leube *et al*. reported a large German pedigree with CD and linkage to the region telomeric to D18S1153 on Chr 18p with a maximal LOD score of 3.17 (34). Follow-up studies narrowed this dystonia locus to a 30 cM region near D18S1098, but also presented evidence of locus heterogeneity in adult-onset CD (16,35). More recent work has shed doubts on the DYT7 locus for CD on Chr 18p (36). Although CD and other forms of adult-onset dystonia are genetically

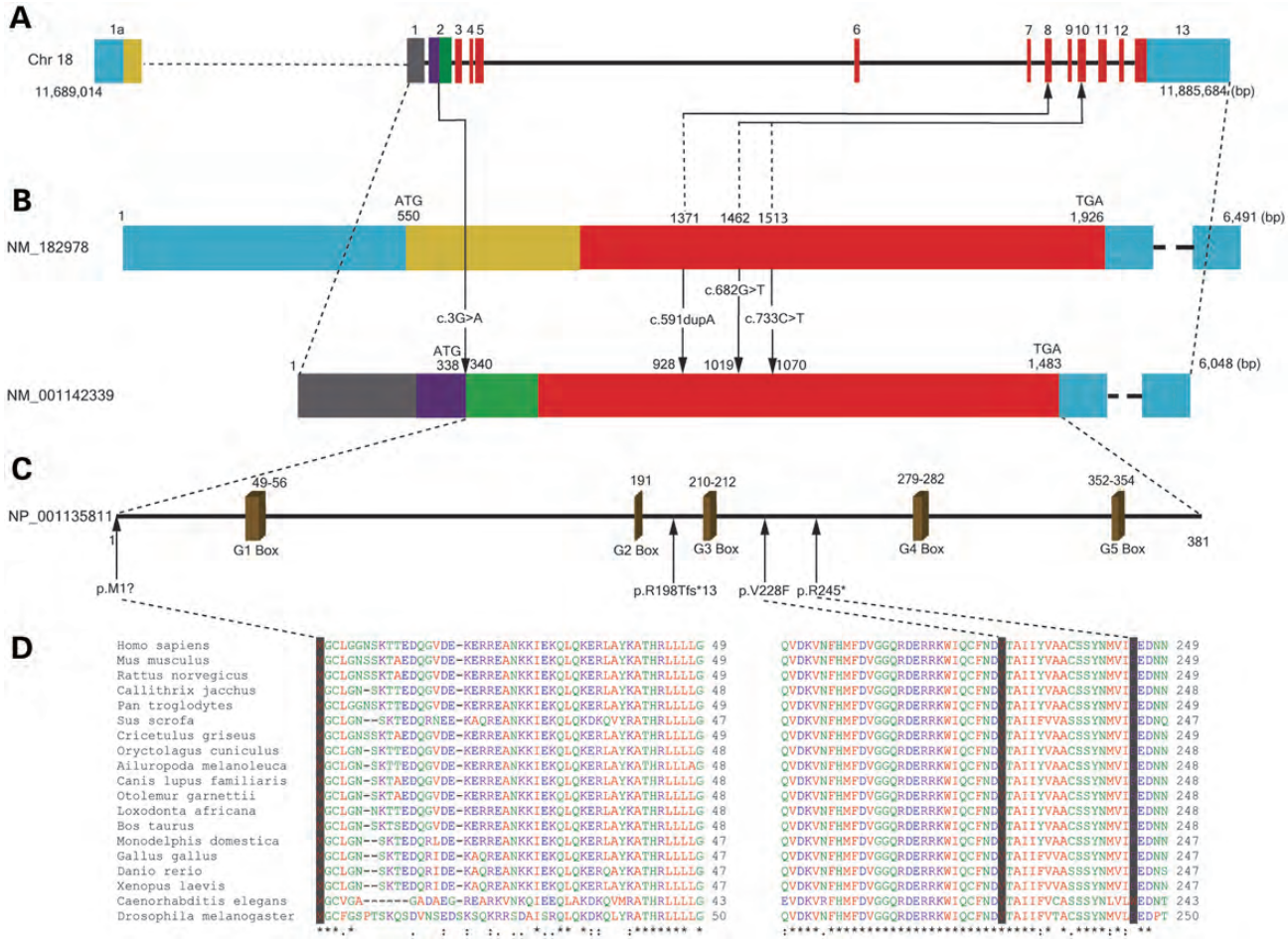

Figure 2. Organization of GNAL gene, transcripts and full-length protein. (**A**) Structure of *GNAL* on Chr 18p presented in the 5′ to 3′ direction showing the location of four identified mutations in probands with dystonia. (**B**) The long and major isoforms of *GNAL* differ at Exon 1. (**C**) Missense mutations in highly conserved regions of Gα(olf) are shown in relationship to GTP binding domains (G1–G5). (**D**) The three Gα(olf) amino acids altered by missense mutations in *GNAL* show conservation in mammals (chimpanzees, marmosets, pigs, mice, rats, hamsters, rabbits, dogs, galagos, elephants, cows, and opossums) non-mammalian vertebrates (chickens, zebrafish, and frogs) and invertebrates (roundworms and fruit flies).

heterogeneous, dystonia is a relatively common manifestation of 18p deletion syndrome (MIM 146390) (27,29–33). Dystonia in 18p deletion syndrome can be focal, segmental or generalized. Some subjects with the 18p deletion syndrome also exhibit myoclonus and white matter abnormalities on magnetic resonance imaging of the brain. Nasir *et al*. (31) identified a Chr 18p 15 Mb deletion that included *GNAL* in a mother and her son both affected with dystonia. Moreover, linkage to Chr 18p was reported in three brothers with late-onset hand-forearm dystonia (28). When integrated with recent work describing several missense and nonsense *GNAL* mutations in familial dystonia (13), the data reported herein indicate that (1) *GNAL* is one dystonia-associated gene on Chr 18p, and (2) Gα(olf) deficiency or dysfunction mainly causes adult-onset CD.

Gα(olf) belongs to a class of GTP-binding proteins (G proteins) which couple G-protein receptors to adenylyl cyclase. Heterotrimeric G protein complexes are composed of three subunits (α, β and γ). G proteins are categorized into four subfamilies according to their α-subunits (Gαs, Gαi/o, Gαq and Gα12). Gα(olf) which has 88% amino acid homology to Gαs is considered to be a member of the Gαs family. Although Gα(olf) was originally discovered in the olfactory neuroepithelium and striatum, it has been identified in pancreatic β-cells, vestibular end organs, testis, spleen, lung and heart (37,38). Our immunohistochemical work indicates that Gα(olf) is widely expressed in brain, especially in motor regions that have previously been associated with dystonia.

At the network level, dystonia has been considered as a disorder of the (1) basal ganglia, (2) olivocerebellar pathways or (3) their interaction (39–41). In dystonic rats, dystonia has been associated with abnormal neurotransmission at the climbing fiber–Purkinje cell synapse (42). Climbing fiber activity leads to the release of CRH which facilitates induction of long-term depression at both parallel fiber and climbing fiber synapses (43). In the striatum, Gα(olf) is upregulated after lesioning the nigrostriatal dopaminergic pathway which contributes to levodopa-induced dyskinesias in models of Parkinson's disease (19). Mutant Gα(olf) and Gα(olf) deficiency may precipitate dystonia by limiting activation of adenylate cyclase in dopamine D1 receptors in striatal medium spiny neurons of the direct pathway (13).

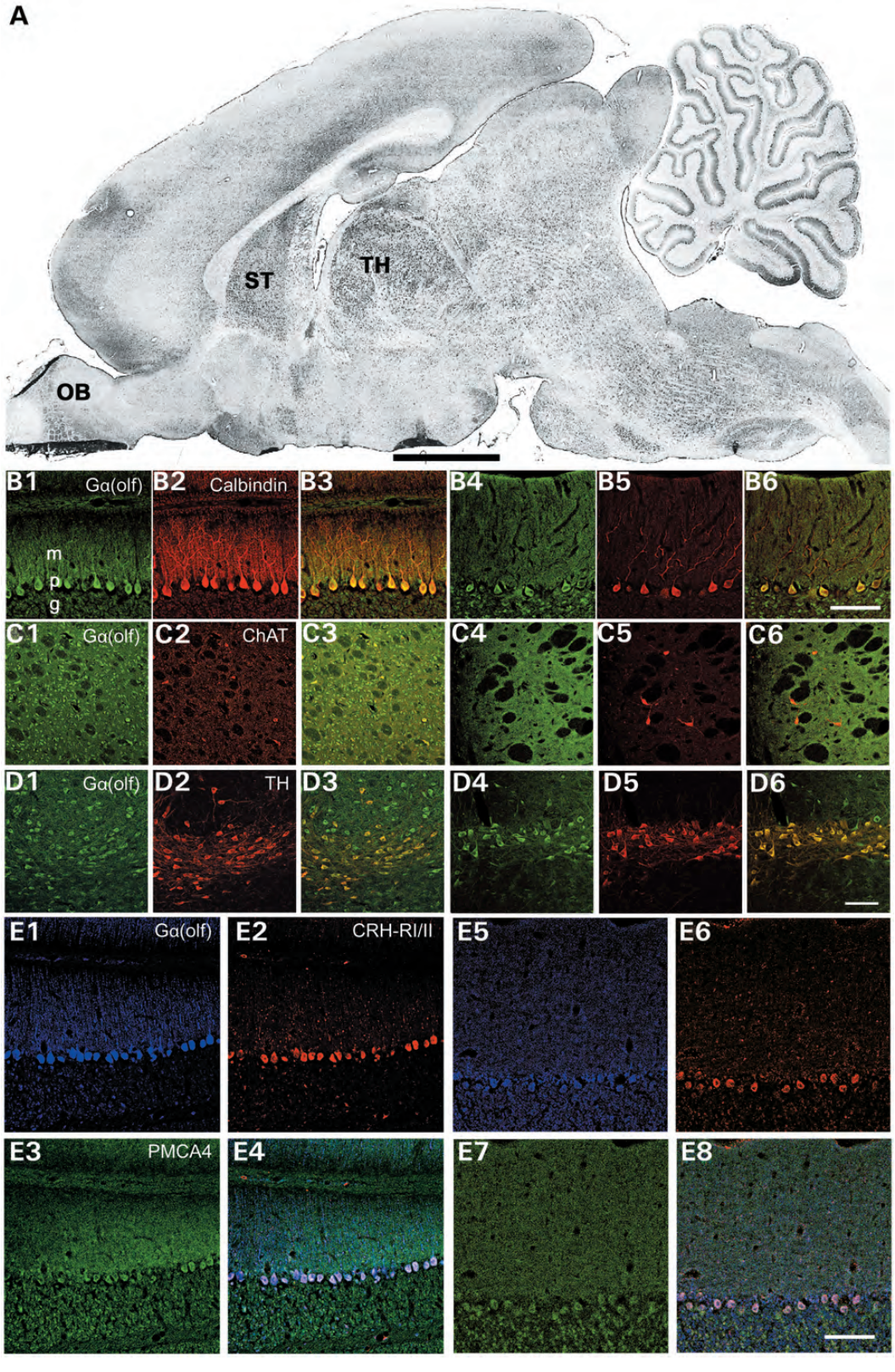

Figure 3. Immunohistochemical localization of Gα(olf) in P14 and adult rat brain. (**A**) Para-sagittal rat brain section. OB, olfactory bulb, ST, striatum. TH, thalamus. (**B1–6**), Double-label fluorescence immunohistochemistry for simultaneous detection of Purkinje cell marker calbindin (red), TH or ChAT (red) with Gα(olf) (green) in P14 (B1-3) and adult (B4-6) rat brain. Gα(olf) -IR was present in ChAT-positive cholinergic neurons in striatum (**C1–6**) and TH-positive dopaminergic neurons in substantia nigra (**D1–6**). (**E1–8**), Triple-label fluorescent immunohistochemistry for simultaneous detection of PMCA4 (green), CRH-RI/II (red) and Gα(olf) (blue) in P14 (E1–4) and adult (E5–8) rat brains. Scale bar, 2 mm for A and 100 μm for the remaining images.

Table 2. Ingenuity pathway analysis—top dysregulated networks

Network	Genes	Score[a]	Focus genes[b]	Top functions
1	*CSTB*, *DMD*, *F13A1*, *FHL3*, *FLOT2*, *FZD3*, *MIR155HG*, *MSX1*, *NFIC*, *NT5C3*, *PABPC3*, *PDE6G*, *SIK3*, *TSC22D1*	24	14	Cell cycle, cellular development, connective tissue development and function
2	*EMR2*, *EXOC6*, *FXYD2*, *HES1*, *IFITM3*, *IKZF1*, *KRTAP17-1*, *LIN7A*, *RAB9A*, *SFMBT2*, *SP140*, *SYT11*	19	12	Cellular development, cellular growth and proliferation, hematological system development and function
3	*AKAP7*, *CERS6*, *CKLF*, *CLINT1*, *HLA-DRB4*, *IL17RB*, *SLC2A8*, *TNFRSF14*, *TPST1*, *TRAF3IP3*	15	10	RNA damage and repair, cell death and survival, gene expression

[a]Network score is the negative log of the *P*-value for the likelihood that network molecules would be found together by chance. Higher scores indicate a greater statistical likelihood that molecules depicted in the network are interconnected.
[b]Number of significantly dysregulated genes associated with that pathway in subjects from Family A with the p.V228F mutation.

Although mutations in *GNAL* had not previously been associated with olfactory dysfunction in humans, two Iranian families with isolated congenital anosmia showed linkage to 18p11.23-q12.2 (44). More importantly, mice deficient in Gα(olf) are anosmic (20). In our study, microsmia was most prominent in those members of African-American Family A also affected with dystonia. However, in the Caucasian families, microsmia was absent or variable in mutation carriers. These data suggest that, like dystonia, the penetrance of olfactory dysfunction may be reduced and dependent on genetic background. In addition, alternate olfactory signaling pathways may compensate for Gα(olf) deficiency given that, in contrast to the Caucasian families, Family A harbored a missense mutation in *GNAL*.

At the cellular level, some forms of primary dystonia have been characterized as neurodevelopmental disorders and several dystonia associated proteins (*THAP1*, *TAF1* and *CIZ1*) play important roles at the G_1–S checkpoint of the cell cycle (2,10,12,45). Similarly, our gene expression studies identified dysregulated cellular networks involved in cell cycle, development and gene expression. Although lymphoblastoid cells do not faithfully model many aspects of neuronal function, most cellular processes are shared and possible links among dystonia-associated proteins should not be ignored. In this regard, administration of the dopamine receptor blocker haloperidol induces prolonged increases in the levels of Ser10 phosphorylated histone H3 in dopamine D2 receptor-expressing neurons of the dorsomedial and the dorsolateral striatum and this effect is mediated through adenosine A2A receptor-mediated activation of Gα(olf) (46,47). Histone H3 phosphorylation at Ser10 inhibits checkpoint kinase 1, a key component of the ATM/ATR arm of the G_1–S checkpoint pathway (48). Therefore, it is conceivable that loss of Gα(olf) function could disturb G_1–S cell cycle control.

MATERIALS AND METHODS

Human subjects

Human studies were conducted in accordance with the Declaration of Helsinki, with formal approval from the institutional review boards at each participating study site. All genetic and phenotypic analyses and publication of the results were approved by the University of Tennessee Health Science Center Institutional Review Board (#01-07346-XP). Enrollment of patients with primary dystonia and neurologically normal controls is described in previous publications (7,12). Genomic DNA was extracted from peripheral whole blood or saliva (Oragene DNA Self-Collection kit, DNA Genotek®, Kanata, Ontario, Canada). Total leukocyte RNA was extracted with the LeukoLOCK™ Total RNA Isolation System (Ambion, Austin, TX, USA) as previously described (7).

Given the established role of Gα(olf) in olfaction and to investigate the potential utility of olfactory testing as a preclinical diagnostic tool in primary dystonia, Families A–D were examined with the 40-item University of Pennsylvania Smell Identification Test (26) (UPSIT; Sensonics, Inc., Haddon Heights, NJ, USA). UPSIT data were analyzed with SAS 9.3 (SAS Institute, Inc., Cary, NC, USA).

Linkage analysis

Eighteen subjects from Family A were genotyped with the HumanLinkage-24 Bead Chip (Illumina, San Diego, CA, USA). SNP genotypes were analyzed with Superlink-Online SNP version 1.0 (http://cbl-hap.cs.technion.ac.il/superlink-snp/) (21) using a dominant model with a mutant allele frequency of 0.0001 and penetrance of 0.5 (Supplementary Material, Table S2).

Exome sequencing and variant analysis

In-solution whole-exome capture and massively parallel sequencing was performed on two definitely affected and one unaffected subject from Family A using the Agilent SureSelect^{XT} All Exon Kit 51 Mb (Santa Clara, CA, USA). Three micrograms of genomic DNA from two affected and one control subject was sheared to yield 100–450 bp fragments. Sheared DNA was then subjected to Illumina paired-end library preparation followed by enrichment for target sequences (Agilent SureSelect^{XT} Automated Target Enrichment for Illumina Paired-End Multiplexed Sequencing). Enriched DNA fragments were sequenced on Illumina's HiSeq 2000 platform as paired-end 100 base reads (Otogenetics Co., Norcross, GA, USA).

Percentage of exome coverage was based on exons targeted by the 51 Mb All Exon v4 kit which incorporates Consensus Coding Sequence (CCDS), NCBI Reference Sequence (RefSeq) and GENCODE annotations. Sequence reads

(FASTQ) were mapped to the human reference genome (NCBI build 37.1) with NextGENe® (SoftGenetics, State College, PA, USA). The average read length for all three samples was 97 nt. To maximize the probability of detecting the causal SV, all base changes occurring in two or more reads in any individual sample were classified as variants for downstream analyses. A variant comparison was done between the two affected and one unaffected subjects to filter down the number of SVs in order to identify the putative causal variant. With NextGENe® software, all filtering parameters were implemented simultaneously: (i) homozygous SVs, (ii) intergenic SVs, (iii) deep intronic SVs ($\geq$12 nt from splice sites), (iv) SVs reported in dbSNP Build 135, (v) synonymous SVs and (vi) non-pathogenic non-synonymous SVs (12,49). In order to filter benign missense variants, the pathogenicity of non-synonymous single amino acid substitutions was interrogated with five *in silico* tools: PolyPhen-2, MutationTaster, $SIFT_{new}$, LRT_{new} (Likelihood Ratio Test) and $PhyloP_{new}$ (50). Conservative scores were employed for filtering: PolyPhen-2 ($\geq$0.5), MutationTaster ($\geq$0.5), $SIFT_{new}$ ($>$0.5), LRT_{new} ($\geq$0.5) and $PhyloP_{new}$ ($\geq$0.8). We retained those SVs that met at least four of these five criteria. Remaining SVs were filtered if identified in two or more subjects included in the 1000 Genomes Project (http://www.1000genomes.org) or Exome Sequencing Project (http://evs.gs.washington.edu/EVS/). Candidate genes were also eliminated if not expressed in brain [Allen Brain Atlas (http://www.brain-map.org/) and BioGPS (http://biogps.org)].

QRT-PCR

For QRT–PCR, leukocyte RNA was reverse transcribed to cDNA with Ambion's RETROscript™ kit using 500 ng of total RNA as a template. The reaction mixture was incubated at 44°C for 1 h and then at 92°C for 10 min. QRT–PCR was performed using the Roche Applied Science (Penzberg, Germany) LightCycler® 480 system with *GNAL* specific primers and Roche Universal ProbeLibrary probes under the following conditions: 95°C for 10 min; 45 cycles at 94°C for 10 s, 60°C for 10 s and 72°C for 20 s. *GNAL*-specific primers, which were designed using the Roche Universal ProbeLibrary Assay Design Center to span at least one intron, showed efficiencies of 92.5–95.9% and R^2 values $>$0.99 (Supplementary Material, Table S9). The *GNAL* primer pairs for all isoforms, Isoform 1 and Isoform 2, generated single amplicons that produced single well-defined bands on agarose gel electrophoresis. Furthermore, Sanger sequencing confirmed the identity of these bands as *GNAL* cDNA. Cyclophilin D was chosen from a panel of six endogenous controls (β-actin, β-tubulin, TATA-binding protein, hypoxanthine-guanine phosphoribosyltransferase, cyclophilin D and S19), since it showed the highest efficiency (97.8%), smallest sample-to-sample variance and generated an R^2 of 0.996. All samples were run in triplicate and median values were employed for statistical analyses.

Adult human whole brain total RNA [FirstChoice® Human Brain Reference RNA (1 mg/ml)] was obtained from Ambion. Fetal human whole brain and adult human cerebral cortex, cerebellum, and substantia nigra total RNA were purchased from Clontech (Mountain View, CA, USA). Striatum total RNA was acquired from Agilent.

Immunohistochemistry

Perfusion-fixed [normal saline-4% paraformaldehyde in 0.1 M phosphate-buffered saline (PBS)] postnatal day 14 (P14) and adult Sprague–Dawley rat brains were sectioned in the mid-sagittal or coronal planes and processed for detection of Gα(olf) with Purkinje cell marker (calbindin D-28K), tyrosine hydroxylase (TH), choline acetyltransferase (ChAT), a parallel fiber marker (PMCA4) and corticotropin releasing hormone receptors I and II (CRH-RI/II) (Supplementary Material, Table S10). After endogenous peroxidases were quenched, slides were blocked and exposed to a primary rabbit polyclonal anti-Gα(olf) antibody (Novus Biologicals, Littleton, CO, USA; 1:100) overnight. After rinsing with PBS, slides were exposed to biotinylated goat anti-rabbit antibody (1:500) for 4 h, followed by rinsing and exposing to streptavidin for 1 h. Labeling was visualized with nickel-intensified 3, 3′-diaminobenzidine solution (Vector, Burlingame, CA, USA). For double-label fluorescent immunohistochemistry, mouse anti-calbindin monoclonal, mouse anti-TH polyclonal or a goat anti-choline acetyltransferase (ChAT) polyclonal antibodies were used in combination with rabbit anti-Gα(olf). The secondary antibodies were Cy2-tagged donkey anti-rabbit, and rhodamine red-X (RRX)-tagged donkey anti-mouse or anti-goat. Sections were incubated with secondary antibodies for 4 h and then rinsed, dehydrated, cleared and coverslipped with 1,3-diethyl-8-phenylxanthine mounting compound (DPX; Sigma-Aldrich, St. Louis, MO, USA). For triple-label fluorescent immunohistochemistry, goat anti-CRH-RI/II polyclonal, mouse anti-PMCA4 monoclonal antibodies were used in combination with rabbit anti-Gα(olf). The secondary antibodies were Cy2-tagged donkey anti-mouse, and rhodamine red-X (RRX)-tagged donkey anti-goat and Cy5-tagged donkey anti-rabbit. Sections were visualized with both epifluorescence (Leica DM 6000B; Wetzlar, Germany) and confocal laser-scanning (Zeiss LSM 710; Thornwood, NY, USA) microscopes.

Lymphoblastoid transformation and RNA extraction

Lymphocytes from four affected carriers and four non-carriers from Family A were transformed to lymphoblastoid cell lines for downstream analysis. To establish lymphoblastoid cell lines, peripheral blood mononuclear cells were separated by centrifugation on a sodium diatrizoate polysucrose gradient and transformed with Epstein-Barr virus (Coriell, Camden, NJ, USA). The lymphoblastoid cell lines were propagated in RPMI-1640 medium (Sigma-Aldrich) supplemented with 20% fetal bovine serum (Sigma-Aldrich) and 2 mM L-glutamine at 37°C in 5% CO_2. Confluent cells (1×10^6 cells/ml) were harvested for RNA isolation. Ambion's TRI Reagent® was used to isolate RNA. The quality of total RNA derived from leukocytes and lymphoblastoid cell lines was accessed with a NanoDrop® ND-1000 spectrophotometer (NanoDrop Technologies, Wilmington, DE, USA), and Agilent 2100 Bioanalyzer using the Agilent RNA 6000 Nano Chip kit.

Gene expression studies

Total RNA from lymphoblastoid cell lines of eight subjects were processed on Illumina® HumanHT-12 v.4 expression microarray platform (Illumina, San Diego, CA, USA), flexible for high-throughput processing of 12 samples per beadchip, to assess the expression levels in each individual specimen. These arrays investigate whole-genome expression, providing coverage for more than 47 000 transcripts and known splice variants across the human transcriptome. Total RNA (200 ng) was processed using the Illumina® TotalPrep™ RNA Amplification kit (Applied Biosystems, Carlsbad, CA, USA) according to the company's protocol. The raw data were processed for errors and quality checks using Illumina's proprietary GenomeStudio® software. Data were normalized and summarized further with GeneSpring GX® 12.0 software (Agilent® Technologies). Unpaired *t*-tests were used to filter significant probes. Probes that were significant at $P \leq 0.05$ with a mean fold change of ≥ 1.5 were retained for downstream analyses.

Enrichment analysis of differentially expressed genes was performed using WebGestalt (http://bioinfo.vanderbilt.edu/webgestalt/) (49). The differentially expressed gene set was compared with the human genome using the hypergeometric test followed by correction for multiple testing using the Benjamini & Hochberg (BH) method at a significance level of 0.05 (FDR < 0.05) (51). Kyoto Encyclopedia of Genes and Genomes (KEGG) pathways were accessed from WebGestalt (52,53). Dysregulated cellular networks were examined with Ingenuity Pathway Analysis (IPA; Ingenuity, Redwood City, CA, USA).

SUPPLEMENTARY MATERIAL

Supplementary Material is available at *HMG* online.

ACKNOWLEDGEMENTS

The authors thank J. Searcy and A. Strongosky for their assistance with collecting clinical data.

Conflict of Interest statement. None declared.

FUNDING

M.S.L. was supported by the Bachmann-Strauss Dystonia & Parkinson Foundation, Dystonia Medical Research Foundation and NIH/NINDS R01 NS069936. A.P. was supported by governmental funding of clinical research within the Swedish National Health Services (ALF-YF) and by the Swedish Parkinson Foundation (Parkinsonfonden). Z.K.W is partially supported by the NIH/NINDS P50 NS072187, Mayo Clinic Florida (MCF) Research Committee and Dystonia Medical Research Foundation.

REFERENCES

1. Fahn, S. (1988) Concept and classification of dystonia. *Adv. Neurol.*, **50**, 1–8.
2. LeDoux, M.S. (2012) The genetics of dystonias. *Adv. Genet.*, **79**, 35–85.
3. LeDoux, M.S. (2012) Dystonia: phenomenology. *Parkinsonism Relat. Disord.*, **18**(Suppl 1), S162–164.
4. Chan, J., Brin, M.F. and Fahn, S. (1991) Idiopathic cervical dystonia: clinical characteristics. *Mov. Disord.*, **6**, 119–126.
5. Marras, C., Van den Eeden, S.K., Fross, R.D., Benedict-Albers, K.S., Klingman, J., Leimpeter, A.D., Nelson, L.M., Risch, N., Karter, A.J., Bernstein, A.L. *et al.* (2007) Minimum incidence of primary cervical dystonia in a multiethnic health care population. *Neurology*, **69**, 676–680.
6. Puschmann, A., Xiao, J., Bastian, R.W., Searcy, J.A., LeDoux, M.S. and Wszolek, Z.K. (2011) An African-American family with dystonia. *Parkinsonism Relat. Disord.*, **17**, 547–550.
7. Xiao, J., Zhao, Y., Bastian, R.W., Perlmutter, J.S., Racette, B.A., Tabbal, S.D., Karimi, M., Paniello, R.C., Wszolek, Z.K., Uitti, R.J. *et al.* (2010) Novel *THAP1* sequence variants in primary dystonia. *Neurology*, **74**, 229–238.
8. Defazio, G., Abbruzzese, G., Girlanda, P., Liguori, R., Santoro, L., Tinazzi, M. and Berardelli, A. (2012) Phenotypic overlap in familial and sporadic primary adult-onset extracranial dystonia. *J. Neurol.*, **259**, 2414–2418.
9. Ozelius, L.J., Hewett, J.W., Page, C.E., Bressman, S.B., Kramer, P.L., Shalish, C., de Leon, D., Brin, M.F., Raymond, D., Corey, D.P. *et al.* (1997) The early-onset torsion dystonia gene (DYT1) encodes an ATP-binding protein. *Nat. Genet.*, **17**, 40–48.
10. Fuchs, T., Gavarini, S., Saunders-Pullman, R., Raymond, D., Ehrlich, M.E., Bressman, S.B. and Ozelius, L.J. (2009) Mutations in the *THAP1* gene are responsible for DYT6 primary torsion dystonia. *Nat. Genet.*, **41**, 286–288.
11. Charlesworth, G., Plagnol, V., Holmstrom, K.M., Bras, J., Sheerin, U.M., Preza, E., Rubio-Agusti, I., Ryten, M., Schneider, S.A., Stamelou, M. *et al.* (2012) Mutations in ANO3 cause dominant craniocervical dystonia: ion channel implicated in pathogenesis. *Am. J. Hum. Genet.*, **91**, 1041–1050.
12. Xiao, J., Uitti, R.J., Zhao, Y., Vemula, S.R., Perlmutter, J.S., Wszolek, Z.K., Maraganore, D.M., Auburger, G., Leube, B., Lehnhoff, K. *et al.* (2012) Mutations in *CIZ1* cause adult-onset primary cervical dystonia. *Ann. Neurol.*, **71**, 458–469.
13. Fuchs, T., Saunders-Pullman, R., Masuho, I., Luciano, M.S., Raymond, D., Factor, S., Lang, A.E., Liang, T.W., Trosch, R.M., White, S. *et al.* (2012) Mutations in *GNAL* cause primary torsion dystonia. *Nat. Genet.*, **45**, 88–92.
14. Hersheson, J., Mencacci, N., Davis, M., MacDonald, H.N., Trabzuni, D., Ryten, M., Pittman, A., Paudel, R., Kara, E., Fawcett, K. *et al.* (2013) Mutations in the autoregulatory domain of β-tubulin 4a cause hereditary dystonia. *Ann. Neurol*. DOI: 10.1002/ana.23832.
15. Ahmad, F., Davis, M.B., Waddy, H.M., Oley, C.A., Marsden, C.D. and Harding, A.E. (1993) Evidence for locus heterogeneity in autosomal dominant torsion dystonia. *Genomics*, **15**, 9–12.
16. Leube, B., Hendgen, T., Kessler, K.R., Knapp, M., Benecke, R. and Auburger, G. (1997) Sporadic focal dystonia in Northwest Germany: molecular basis on chromosome 18p. *Ann. Neurol.*, **42**, 111–114.
17. Norgren, N., Mattson, E., Forsgren, L. and Holmberg, M. (2011) A high-penetrance form of late-onset torsion dystonia maps to a novel locus (DYT21) on chromosome 2q14.3-q21.3. *Neurogenetics*, **12**, 137–143.
18. Valente, E.M., Bentivoglio, A.R., Cassetta, E., Dixon, P.H., Davis, M.B., Ferraris, A., Ialongo, T., Frontali, M., Wood, N.W. and Albanese, A. (2001) DYT13, a novel primary torsion dystonia locus, maps to chromosome 1p36.13--36.32 in an Italian family with cranial-cervical or upper limb onset. *Ann. Neurol.*, **49**, 362–366.
19. Alcacer, C., Santini, E., Valjent, E., Gaven, F., Girault, J.A. and Herve, D. (2012) Galpha(olf) mutation allows parsing the role of cAMP-dependent and extracellular signal-regulated kinase-dependent signaling in L-3,4-dihydroxyphenylalanine-induced dyskinesia. *J. Neurosci.*, **32**, 5900–5910.
20. Belluscio, L., Gold, G.H., Nemes, A. and Axel, R. (1998) Mice deficient in G(olf) are anosmic. *Neuron*, **20**, 69–81.
21. Silberstein, M., Tzemach, A., Dovgolevsky, N., Fishelson, M., Schuster, A. and Geiger, D. (2006) Online system for faster multipoint linkage analysis via parallel execution on thousands of personal computers. *Am. J. Hum. Genet.*, **78**, 922–935.
22. Larkin, M.A., Blackshields, G., Brown, N.P., Chenna, R., McGettigan, P.A., McWilliam, H., Valentin, F., Wallace, I.M., Wilm, A., Lopez, R. *et al.* (2007) Clustal W and Clustal X version 2.0. *Bioinformatics*, **23**, 2947–2948.

23. Adzhubei, I.A., Schmidt, S., Peshkin, L., Ramensky, V.E., Gerasimova, A., Bork, P., Kondrashov, A.S. and Sunyaev, S.R. (2010) A method and server for predicting damaging missense mutations. *Nat. Methods*, **7**, 248–249.
24. Ng, P.C. and Henikoff, S. (2001) Predicting deleterious amino acid substitutions. *Genome Res.*, **11**, 863–874.
25. Schwarz, J.M., Rodelsperger, C., Schuelke, M. and Seelow, D. (2010) MutationTaster evaluates disease-causing potential of sequence alterations. *Nat. Methods*, **7**, 575–576.
26. Doty, R.L., Shaman, P. and Dann, M. (1984) Development of the University of Pennsylvania Smell Identification test: a standardized microencapsulated test of olfactory function. *Physiol. Behav.*, **32**, 489–502.
27. Awaad, Y., Munoz, S. and Nigro, M. (1999) Progressive dystonia in a child with chromosome 18p deletion, treated with intrathecal baclofen. *J. Child Neurol.*, **14**, 75–77.
28. Bhidayasiri, R., Jen, J.C. and Baloh, R.W. (2005) Three brothers with a very-late-onset writer's cramp. *Mov. Disord.*, **20**, 1375–1377.
29. Graziadio, C., Rosa, R.F., Zen, P.R., Pinto, L.L., Barea, L.M. and Paskulin, G.A. (2009) Dystonia, autoimmune disease and cerebral white matter abnormalities in a patient with 18p deletion. *Arq. Neuropsiquiatr.*, **67**, 689–691.
30. Kowarik, M.C., Langer, S., Keri, C., Hemmer, B., Oexle, K. and Winkelmann, J. (2011) Myoclonus-dystonia in 18p deletion syndrome. *Mov. Disord.*, **26**, 560–561.
31. Nasir, J., Frima, N., Pickard, B., Malloy, M.P., Zhan, L.P. and Grunewald, R. (2006) Unbalanced whole arm translocation resulting in loss of 18p in dystonia. *Mov. Disord.*, **21**, 859–863.
32. Postma, A.G., Verschuuren-Bemelmans, C.C., Kok, K. and van Laar, T. (2009) Characteristics of dystonia in the 18p deletion syndrome, including a new case. *Clin. Neurol. Neurosurg.*, **111**, 880–882.
33. Tezzon, F., Zanoni, T., Passarin, M.G. and Ferrari, G. (1998) Dystonia in a patient with deletion of 18p. *Ital. J. Neurol. Sci.*, **19**, 90–93.
34. Leube, B., Rudnicki, D., Ratzlaff, T., Kessler, K.R., Benecke, R. and Auburger, G. (1996) Idiopathic torsion dystonia: Assignment of a gene to chromosome 18p in a German family with adult onset, autosomal dominant inheritance and purely focal distribution. *Hum. Mol. Genet.*, **5**, 1673–1677.
35. Klein, C., Ozelius, L.J., Hagenah, J., Breakefield, X.O., Risch, N.J. and Vieregge, P. (1998) Search for a founder mutation in idiopathic focal dystonia from northern Germany. *Am. J. Hum. Genet.*, **63**, 1777–1782.
36. Winter, P., Kamm, C., Biskup, S., Kohler, A., Leube, B., Auburger, G., Gasser, T., Benecke, R. and Muller, U. (2012) DYT7 gene locus for cervical dystonia on chromosome 18p is questionable. *Mov. Disord.*, **27**, 1820–1822.
37. Regnauld, K.L., Leteurtre, E., Gutkind, S.J., Gespach, C.P. and Emami, S. (2002) Activation of adenylyl cyclases, regulation of insulin status, and cell survival by G alpha olf in pancreatic beta-cells. *Am. J. Physiol. Regul. Integr. Comp. Physiol.*, **282**, R870–R880.
38. Wackym, P.A., Cioffi, J.A., Erbe, C.B. and Popper, P. (2005) G-protein Golfalpha (GNAL) is expressed in the vestibular end organs and primary afferent neurons of Rattus norvegicus. *J. Vestib. Res.*, **15**, 11–15.
39. Neychev, V.K., Fan, X., Mitev, V.I., Hess, E.J. and Jinnah, H.A. (2008) The basal ganglia and cerebellum interact in the expression of dystonic movement. *Brain*, **131**, 2499–2509.
40. Argyelan, M., Carbon, M., Niethammer, M., Ulug, A.M., Voss, H.U., Bressman, S.B., Dhawan, V. and Eidelberg, D. (2009) Cerebellothalamocortical connectivity regulates penetrance in dystonia. *J. Neurosci.*, **29**, 9740–9747.
41. LeDoux, M.S. (2011) Animal models of dystonia: lessons from a mutant rat. *Neurobiol. Dis.*, **42**, 152–161.
42. LeDoux, M.S. and Lorden, J.F. (2002) Abnormal spontaneous and harmaline-stimulated Purkinje cell activity in the awake genetically dystonic rat. *Exp. Brain Res.*, **145**, 457–467.
43. Ohtsuki, G., Piochon, C. and Hansel, C. (2009) Climbing fiber signaling and cerebellar gain control. *Front Neurosci.*, **3**, 4.
44. Ghadami, M., Majidzadeh, A.K., Morovvati, S., Damavandi, E., Nishimura, G., Komatsu, K., Kinoshita, A., Najafi, M.T., Niikawa, N. and Yoshiura, K. (2004) Isolated congenital anosmia with morphologically normal olfactory bulb in two Iranian families: a new clinical entity? *Am. J. Med. Genet. A.*, **127A**, 307–309.
45. Makino, S., Kaji, R., Ando, S., Tomizawa, M., Yasuno, K., Goto, S., Matsumoto, S., Tabuena, M.D., Maranon, E., Dantes, M. *et al.* (2007) Reduced neuron-specific expression of the TAF1 gene is associated with X-linked dystonia-parkinsonism. *Am. J. Hum. Genet.*, **80**, 393–406.
46. Bertran-Gonzalez, J., Hakansson, K., Borgkvist, A., Irinopoulou, T., Brami-Cherrier, K., Usiello, A., Greengard, P., Herve, D., Girault, J.A., Valjent, E. *et al.* (2009) Histone H3 phosphorylation is under the opposite tonic control of dopamine D2 and adenosine A2A receptors in striatopallidal neurons. *Neuropsychopharmacology*, **34**, 1710–1720.
47. Rodriguez-Collazo, P., Snyder, S.K., Chiffer, R.C., Zlatanova, J., Leuba, S.H. and Smith, C.L. (2008) cAMP signaling induces rapid loss of histone H3 phosphorylation in mammary adenocarcinoma-derived cell lines. Exp. Cell *Res.*, **314**, 1–10.
48. Liokatis, S., Stützer, A., Elsässer, S.J., Theillet, F.X., Klingberg, R., van Rossum, B., Schwarzer, D., Allis, C.D., Fischle, W. and Selenko, P. (2012) Phosphorylation of histone H3 Ser10 establishes a hierarchy for subsequent intramolecular modification events. *Nat. Struct. Mol. Biol.*, **19**, 819–823.
49. Zhang, B., Kirov, S. and Snoddy, J. (2005) WebGestalt: an integrated system for exploring gene sets in various biological contexts. *Nucleic Acids Res.*, **33**, W741–748.
50. Liu, X., Jian, X. and Boerwinkle, E. (2011) dbNSFP: a lightweight database of human nonsynonymous SNPs and their functional predictions. *Hum. Mutat.*, **32**, 894–899.
51. Benjamini, Y. and Hochberg, Y. (1995) Controlling the false discovery rate - a practical and powerful approach to multiple testing. *J. Roy. Stat. Soc. Ser. B. Met.*, **57**, 289–300.
52. Ashburner, M., Ball, C.A., Blake, J.A., Botstein, D., Butler, H., Cherry, J.M., Davis, A.P., Dolinski, K., Dwight, S.S., Eppig, J.T. *et al.* (2000) Gene ontology: tool for the unification of biology. The Gene Ontology Consortium. *Nat. Genet.*, **25**, 25–29.
53. Kanehisa, M. and Goto, S. (2000) KEGG: kyoto encyclopedia of genes and genomes. *Nucleic Acids Res.*, **28**, 27–30.